Sensors and Actuators A 192 (2013) 140–144

Contents lists available at SciVerse ScienceDirect

Sensors and Actuators A: Physical

journal homepage: www.elsevier.com/locate/sna

Nanogaps controlled by liquid nitrogen freezing and the effects on hydrogen gas sensor performance

Taehoo Chang[1], Hwaebong Jung[1], Byungjin Jang, Junmin Lee, Jin-Seo Noh*, Wooyoung Lee*

Department of Materials Science and Engineering, Yonsei University, 50 Yonseiro, Seodaemun-gu, Seoul 120-749, Republic of Korea

ARTICLE INFO

Article history:
Received 3 July 2012
Received in revised form 4 December 2012
Accepted 8 December 2012
Available online 20 December 2012

Keywords:
Palladium (Pd)
Hydrogen gas (H_2)
Polydimethylsiloxane (PDMS)
Nanogap
Liquid nitrogen

ABSTRACT

A practical strategy for the reduction of nanogap width has been investigated using liquid nitrogen freezing of Pd-sputtered elastomeric substrates. Two types of hydrogen gas sensors, in which no pre-strain and 25% elongation were applied to Pd films on the elastomeric substrates, showed extremely low detection limits of less than 300 and 200 ppm, respectively, after liquid nitrogen freezing and recovery to room temperature. For the non-strained sensors, the nanogap width was measured to be about 90 nm, whereas it was more reduced to 25 nm on the elongated sensors. Both sensors exhibited perfect On–Off switching, fast response, and good reversibility, which are based on the nanogap open–close mechanism upon exposure to hydrogen gas. These results provide a valuable clue for reducing nanogap width, thereby improving the hydrogen-sensing capabilities of nanogap-based On–Off hydrogen sensors.

1. Introduction

With the rapid progress in the design of chemical sensors over the past several decades, nanoscale gaps have been of great interest to researchers interested in improving the sensing performance such as response time, sensitivity, and selectivity [1–4]. Various strategies to create nanogaps have been studied, but complicated and costly fabrication processes remained one of the biggest challenges to be addressed. In hydrogen gas (H_2) sensors, palladium (Pd) nanogap-based sensors have witnessed great advances in nanogap design, which have enabled perfect On–Off sensing and rapid, precise, and selective H_2 detection [5–13]. However, some disadvantages, like poor detection limit and complex fabrication methods, have been obstacles to the commercialization of optimum H_2 sensors. To tackle these issues, we previously reported on nanogap-based H_2 sensors which used an elastomeric substrate [14,15]. Note that nanogaps were generated by either stretching the Pd film on an elastomeric substrate or by simple exposure to hydrogen, methods referred to as highly mobile thin films on an elastomeric substrate (MOTIFE) and cracked Pd films on an elastomeric substrate (CPE), respectively. Both sensors showed perfect On–Off behavior, good reliability, and rapid response of less than 1s. In addition, those are considered to be important strategies for making nanogaps by the use of facile, low cost, scalable, and lithography-free methods. However, the reduction of nanogap widths, which is highly related to the detection limit of nanogap-based H_2 sensors, has not been sufficiently explored. In this regard, even though several papers reported successful control of the nanogap size to below 100 nm by using top-down approaches like focused ion beam milling [16], lowering the detection limit below 0.1% H_2 could not be realized.

Here, we report a practical method for reduction of the nanogap width to below 100 nm in Pd films on an elastomeric substrate using liquid nitrogen freezing (LNF). Nanogaps are formed in two different ways. In the first sample (sample A), no pre-strain is applied and random cracks are created after LNF due to a difference in thermal expansion coefficients between polydimethylsiloxane (PDMS) and Pd, while 25% elongation by stretching generates cracks before LNF for the other type of sample (sample B). For both types of sensors, LNF contributes to reduction of nanogap widths by restricting recovery of cracked Pd to an equilibrium dimension upon exposure to H_2. This easy approach to reduce nanogap widths enables the sensors to show On–Off behavior with a very low detection limit.

2. Experiments

The elastomeric substrates were fabricated by mixing PDMS elastomer (Sylgard 184 Silicon Elastomer Base, Dow Corning) with a curing agent (weight ratio = 10:1), followed by curing at 75 °C for 3 h. The PDMS substrate thickness was 0.80 mm and its size was 20 mm × 10 mm. In the next step, the PDMS substrate was covered with a 10 nm-thick Pd film using direct current (DC) magnetron

* Corresponding authors. Tel.: +82 2 21232834; fax: +82 2 312 5375.
E-mail addresses: jinseonoh@yonsei.ac.kr (J.-S. Noh), wooyoung@yonsei.ac.kr (W. Lee).
[1] These authors equally contributed to this work.

0924-4247/$ – see front matter © 2012 Elsevier B.V. All rights reserved.
http://dx.doi.org/10.1016/j.sna.2012.12.009

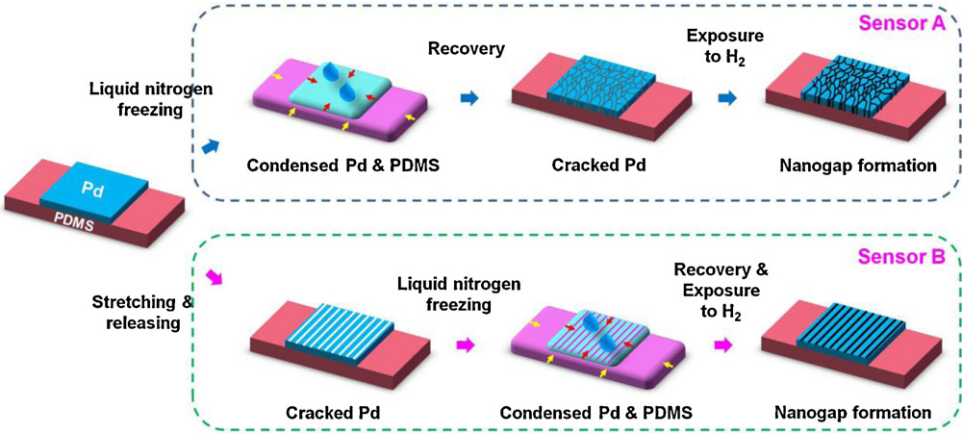

Fig. 1. Schematic fabrication processes for two types of sensors. No pre-strain is applied to the Pd/PDMS before LNF for sensor A, while the Pd/PDMS is elongated by 25% before LNF for sensor B.

sputtering. The Pd film size was 10 mm × 10 mm. The chamber was kept under ultra-high vacuum (4×10^{-8} Torr) before Pd deposition and the working pressure was 2×10^{-6} Torr. Pd deposition was conducted under an Ar flow of 14 sccm (purity: 99.9999%) at a DC power of 20 W by the use of a highly pure Pd target (purity: 99.99%) [15].

After all samples went through these processes, they were divided into two different categories. For half the samples, 2–3 liquid nitrogen droplets were dropped on the Pd film. The other samples were put under a tensile strain (25% in this case) exerted by a tensile machine, then liquid nitrogen was dropped on the Pd film. The processed films were brought under a scanning electron microscope (SEM, JEOL Ltd., JSM-6500F) and an optical microscope (OM, Olympus Co.) for close examination of surface morphologies.

The H_2 sensing system consisted of a gas chamber with a capacity of 250 ml and H_2 and N_2 mass flow controllers. The gas chamber was equipped with a gas inlet and outlet, and a gas mixture of H_2 and N_2 flowed into it through the inlet after the gases were intermixed at a desired ratio. When the chamber pressure was higher than ambient pressure, a check valve opened, thus the chamber was kept constant at ambient pressure. The purity of both H_2 and N_2 gases was 99.9%. The real-time electrical resistance or

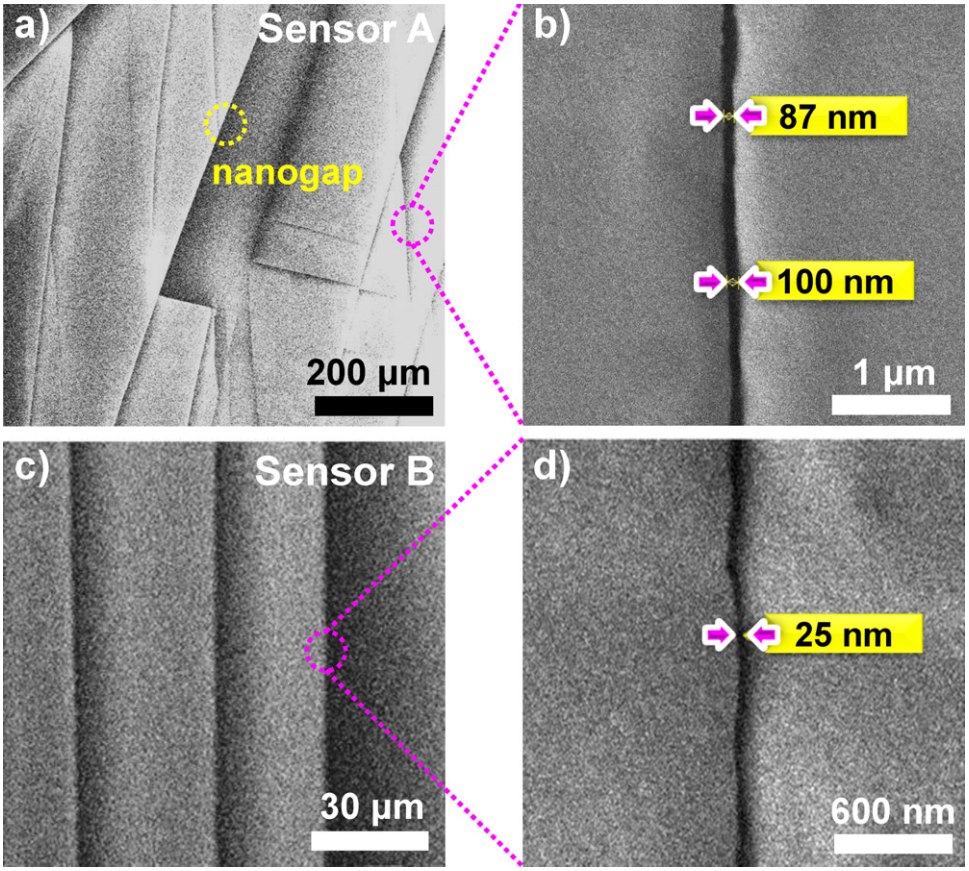

Fig. 2. SEM images of nanogaps formed in (a) sensor A and (c) sensor B. (b) and (d) are zoom-in images for selected parts of sensors A and B, respectively. For both sensors, the width of nanogaps is shown to be less than 100 nm.

current change upon flowing H_2 was monitored at room temperature using a current source-measure unit (Keithley 236) and a nanovoltmeter (Keithley 2182) that were connected to a personal computer [15].

3. Results and discussion

Schematic fabrication procedures for sensors A and B are shown in Fig. 1. For both sensors, the dimensions of the PDMS substrate were identical (20 mm long, 10 mm wide, and 0.8 mm thick) and the thickness of the Pd film was fixed at 10 nm, which was the optimum thickness reported in our previous works [14,17]. The only distinction between the two processes is the presence or absence of a sample-stretching step before the LNF step. This results in differences in temporal points and overall patterns of crack generation. The cracks are generally created in Pd/PDMS structures due to a surface property change of PDMS from a soft surface to a silica-like brittle surface during Pd sputtering [18,19]. This brittle surface is vulnerable to internal or external stresses such as constriction, elongation, and torsion. For sensor A, where no prestrain was applied, cracks are created by the different magnitudes of recovery between the Pd film and PDMS substrate after LNF. This process relies on the larger coefficient of thermal expansion (CTE) of PDMS compared with that of Pd [20–22]. First, the LNF process applies a compressive and tensile strain onto the surface of Pd and PDMS, respectively, due to the larger CTE of PDMS. Then, the PDMS substrate tends to recover more swiftly to a larger extent than the Pd film, leading to a tensile strain on the Pd film and the consequent generation of cracks. These cracks are random in nature since the stress distribution during LNF and the recovery processes is somewhat irregular. The subsequent steps (exposure to H_2 followed by N_2 ventilation) make the generated cracks become stable nanogaps with optimal gap widths. On the other hand, cracks are generated by simply stretching the Pd/PDMS for sensor B. The broken Pd films recontact each other after releasing from elongation, leaving behind closed cracks. These closed cracks were transformed into open nanogaps through the process of recovery to the equilibrium dimensions of the cracked Pd films after exposure to H_2. A LNF step inserted between the crack generation and H_2 flow steps plays an important role in the reduction of nanogap width because the broken Pd films can become more overlapped. The size of the cracks on the surface of the PDMS substrate is more likely to constrict during this step, which leads to narrower nanogaps after the H_2 flow/recovery cycles. The effects of LNF on nanogap width and H_2 sensing properties are discussed in further detail below.

SEM images of sensors A and B fabricated following the above schemes are shown in Fig. 2. As depicted in Fig. 1, random nanogaps appear on the surface of sensor A, possibly due to the irregular internal stress distribution developed during the LNF and recovery processes. The center-to-center distance between nanogaps was about $200 \pm 150\,\mu m$ (Fig. 2(a)). From the enlarged image of a selected nanogap line, the average width of the randomly distributed nanogaps was estimated to be 80–120 nm, as shown in Fig. 2(b). In contrast, sensor B shows linear nanogaps on its surface that are oriented perpendicular to the stretching direction, as shown in Fig. 2(c). The center-to-center distance between adjacent nanogaps was approximately $30 \pm 10\,\mu m$, corresponding to 10–20% of that of sensor A. This may be because the 25% uniaxial strain transferred more stress to the Pd/PDMS interface than the LNF process internally did, generating more crack initiation points on sensor B. The average width of the nanogaps was approximately 25 nm, as shown in Fig. 2(d), which is more than 10-fold smaller than that of the nanogaps formed by only simple stretching. This substantial reduction in nanogap width is attributed to the contraction of the initial cracks and broken Pd films during the LNF process, verifying the efficacy of the LNF process as a facile approach to achieve sub-100 nm nanogaps.

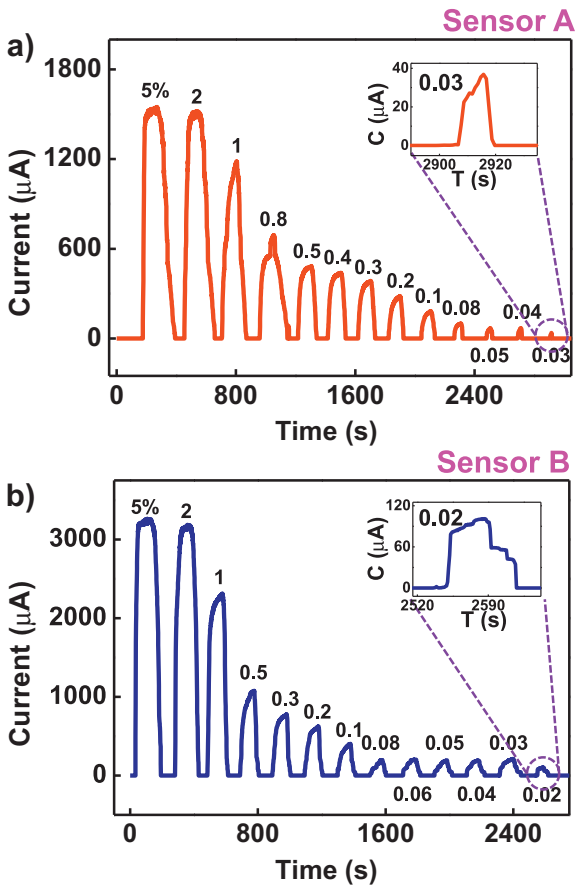

Fig. 3. Real-time electrical responses of (a) sensor A and (b) sensor B at room temperature. Electric currents were measured in response to H_2 concentrations varying in the range of 5% to a detection limit. The insets of (a) and (b) show response curves of the respective sensors at lowest detectable H_2 concentrations, i.e., 300 and 200 ppm.

To examine the effects of the reduced nanogaps on H_2 sensing performance, the real-time electrical responses with gradually decreasing H_2 concentrations were measured for both types of sensors. The results are shown in Fig. 3. Both sensors operate in perfect On–Off mode over the entire H_2 concentration range, indicating that the closed (On state)–open (Off state) mechanism of the nanogaps functions well in accordance with H_2 absorption/desorption processes. The apparent On–Off behaviors of the sensors also eliminate concerns about the possibility of being transformed into On-type sensors in the sub-100 nm regime. The current level generally varies in a stepwise manner corresponding to H_2 concentrations in the range of 2% to the detection limit. This demonstrates the scalability of our sensors to H_2 concentration. The close current levels for H_2 concentrations of 2 and 5% may result from the fact that the largest volume expansion in Pd films is accompanied by a phase transition of Pd from the α to the β phase, which occurs slightly below 2% H_2 [23–25]. This reasoning is further supported by the finding that the current level changes the most between 2 and 0.8% (or 0.5%), in which the phase of Pd changes from a mixture of α and β phases to only β phase. The response time, defined as the time to reach 90% of the total change in electrical resistance, is also found to be short: <1 s over most measured H_2 concentrations for both sensors. This value is comparable to the response times previously reported for Pd nanogap-based H_2 sensors fabricated by just stretching [14]. The most surprising result for the sensors

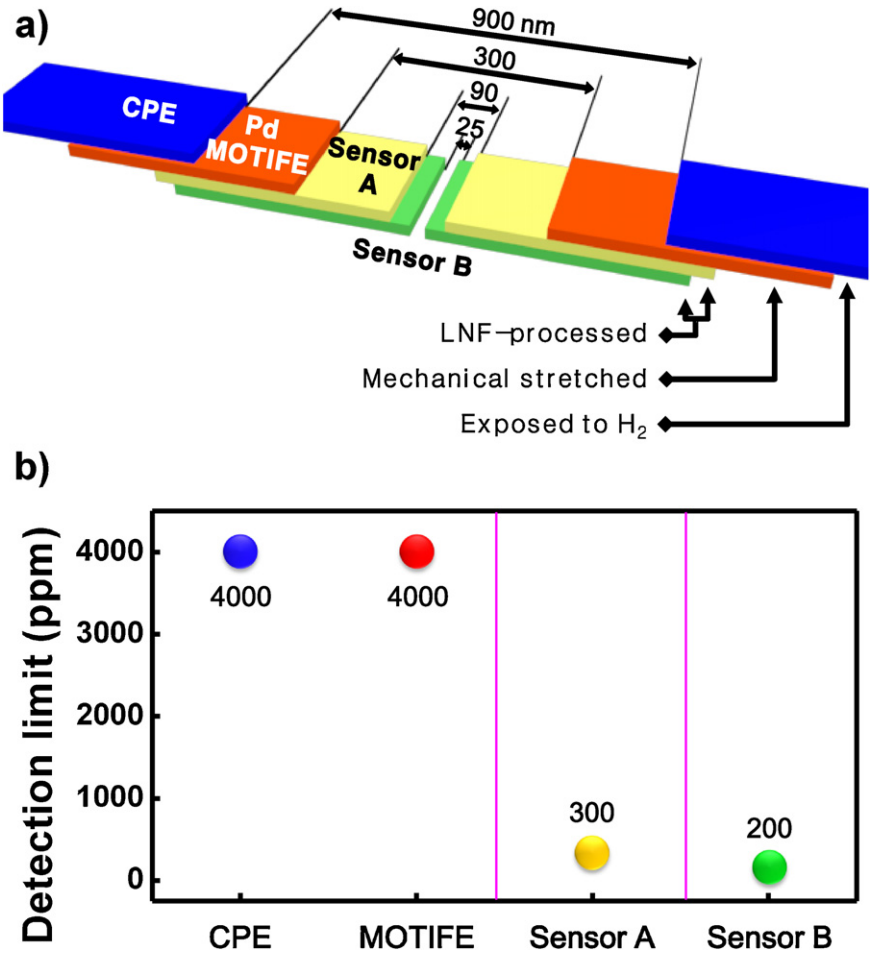

Fig. 4. Comparison of (a) nanogap widths and (b) detection limits between the previously reported nanogap-based sensors (CPE and Pd MOTIFE) [14,15] and the current LNF-processed sensors (sensors A and B). The detection limit is found to be substantially lowered in accordance with the reduction in the nanogaps.

having undergone the LNF process is that the lowest detectable H_2 concentrations, simply termed H_2 detection limits, are 300 and 200 ppm for sensors A and B, respectively, as shown in the insets of Fig. 3. These were drastically reduced from the detection limits of previously reported Pd nanogap-based H_2 sensors [14,15]. This result provides a simple means to make more promising H_2 sensors based on Pd nanogaps, as the poor detection limit has been one of the biggest hurdles to overcome for these sensors to meet high-performance standards.

The comparisons of nanogap widths and detection limits between Pd nanogap-based H_2 sensors are summarized in Fig. 4. Representative prior nanogap sensors formed on Pd films, i.e., CPE and Pd MOTIFE, exhibited average nanogap widths of 900 and 300 nm, respectively, as shown in Fig. 4(a) [14,15]. These large widths led to a relatively high detection limit of 4000 ppm, as shown in Fig. 4(b). Provided that the nanogap width is reduced to 90 nm (sensor A), the detection limit is drastically reduced to 300 ppm. A further decrease in nanogap width to 25 nm (sensor B) results in an even lower detection limit (200 ppm). Although the relationship between the nanogap width and detection limit is not linear, Fig. 4 clearly shows a general dependence of detection limit on nanogap width. The wide nanogaps of the previous sensors require high H_2 concentrations (>4000 ppm) to be closed by volume expansion of broken Pd films since some amount of β phase is required to appear for this physical event. In contrast, the much narrower nanogaps of the LNF-processed sensors can be closed by the minimal volume expansion that is triggered by H_2 absorption at low concentrations (<300 ppm), where Pd may stay in the α phase.

4. Conclusions

Sub-100 nm nanogaps were fabricated in Pd films on an elastomeric substrate (PDMS), using a liquid nitrogen freezing (LNF) process. Two types of sensors were prepared using slightly different methods, in which the Pd film was either non-strained (sensor A) or pre-strained (sensor B) before the LNF. The nanogaps appeared to be oriented perpendicular to the straining direction in sensor B, while they were random in sensor A. Sensor B showed very narrow nanogaps with an average width of 25 nm and a shorter nanogap-to-nanogap distance than that of sensor A. This width is more than 10-fold smaller compared with sensors fabricated previously by just stretching, indicating the LNF process effectively constricts the Pd/PDMS structure and the generated cracks. Both types of sensors behaved in a perfect On–Off manner and showed a short response time (<1 s) and good scalability to H_2 concentrations. Most surprisingly, the LNF-processed sensors achieved a very low detection limit, down to 200 ppm, which has never been achieved with Pd nanogap-based H_2 sensors. These results reflect that the shrunken nanogaps enabled by the LNF process can detect trace amounts of H_2 swiftly and precisely, while retaining the On–Off operability. Furthermore, both the straining technique and the LNF

process can be easily applied to large-scale thin film processes at low cost, increasing the possibility that H_2 sensors based on narrow nanogaps will be commercialized.

Acknowledgments

This work was supported by the Priority Research Centers Program through the National Research Foundation of Korea (NRF) funded by the Ministry of Education, Science and Technology (2009-0093823) and by the Converging Research Center Program through the Ministry of Education, Science, and Technology (No. 2010K001430).

References

[1] D. Porath, A. Bezryadin, S. Vries, C. Dekker, Direct measurement of electrical transport through DNA molecules, Nature 403 (2000) 635–638.
[2] C. Chen, F. Ko, C. Chen, T. Liu, E. Chang, Electrical signal amplification of DNA hydridization by nanoparticles in a nanoscale gap, Applied Physics Letters 91 (2007) 253103.
[3] S. Roy, Z. Gao, Nanostructure-based electrical biosensors, Nano Today 4 (2009) 318–334.
[4] M. Spencer, I. Yarovsky, W. Wlodarski, K. Kalantar-zadeh, Interaction of hydrogen with zinc oxide nanorods: why the spacing is important, Nanotechnology 22 (2011) 135704.
[5] F. Favier, E.C. Walter, M.P. Zach, T. Benter, R.M. Penner, Hydrogen sensors and switches from electrodeposited palladium mesowire arrays, Science 293 (2001) 2227–2231.
[6] S. Mubeen, B. Yoo, N.V. Myung, Fabrication of nanoelectrodes and nanojunction hydrogen sensor, Applied Physics Letters 93 (2008) 133111.
[7] F.J. Ibanez, F.P. Zamborini, Reactivity of hydrogen with solid-state films of alkylamine- and tetraoctylammonium bromide-stabilized Pd, PdAg, and PdAu nanoparticles for sensing and catalysis applications, Journal of the American Chemical Society 130 (2008) 622–633.
[8] E.C. Walter, F. Favier, R.M. Penner, Palladium mesowire arrays for fast hydrogen sensors and hydrogen-actuated switches, Analytical Chemistry 74 (2002) 1546–1553.
[9] F. Yang, D.K. Taggart, R.M. Penner, Fast, sensitive hydrogen gas detection using single palladium nanowires that resist fracture, Nano Letters 9 (2009) 2177–2182.
[10] S. Cherevko, N. Kulyk, J. Fu, C. Chung, Hydrogen sensing performance of electrodeposited conoidal palladium nanowire and nanotube arrays, Sensors and Actuators B 136 (2009) 388–391.
[11] M. Khanuja, S. Kala, B.R. Mehta, F.E. Kruis, Concentration-specific hydrogen sensing behavior in monosized Pd nanoparticle layers, Nanotechnology 20 (2009) 015502.
[12] T. Kiefer, L.G. Villanueva, F. Fargier, F. Favier, J. Brugger, Fast and robust hydrogen sensors based on discontinuous palladium films on polyimide, fabricated on a wafer scale, Nanotechnology 21 (2010) 505501.
[13] M.Z. Atashbar, D. Banerji, S. Singamaneni, Room-temperature hydrogen sensor based on palladium nanowires, IEEE Sensors Journal 5 (2005) 792–797.
[14] J. Lee, W. Shim, E. Lee, J. Noh, W. Lee, Highly mobile palladium thin films on an elastomeric substrate, Angewandte Chemie International Edition 50 (2011) 5301–5305.
[15] J. Lee, J. Noh, S. Lee, B. Song, H. Jung, W. Kim, W. Lee, Cracked palladium films on an elastomeric substrate for use as hydrogensensors, International Journal of Hydrogen Energy 37 (2012) 7934–7939.
[16] T. Kiefer, F. Favier, O. Vazquez-Mena, G. Villanueva, J. Brugger, A single nanotrench in a palladium microwire for hydrogen detection, Nanotechnology 19 (2008) 125502.
[17] G. Frazier, R. Glosser, Characterization of thin films of the palladium–hydrogen system, Journal of the Less-Common Metals 74 (1980) 89–96.
[18] M.J. Owen, P.J. Smith, Plasma treatment of polydimethyl-siloxane, Journal of Adhesion Science and Technology 8 (1994) 1063–1075.
[19] D. Fuard, T. Tzvetkova-Chevolleau, S. Decossas, P. Tracqui, P. Schiavone, Optimization of poly-di-methyl-siloxane (PDMS) substrates for studying cellular adhesion and motility, Microelectronic Engineering 85 (2008) 1289–1293.
[20] J.S. Elizabeth, D.D. Michael, M.W. George, C. Federico, A technique to transfer metallic nanoscale patterns to small and non-planar surfaces, ACS Nano 3 (2009) 59–65.
[21] W.W. Tooley, S. Feghhi, S.J. Han, J. Wang, N.J. Sniadecki, Thermal fracture of oxidized polydimethylsiloxane during soft lithography of nanopost arrays, Journal of Micromechanics and Microengineering 21 (2011) 054013.
[22] F.C. Nix, D. MacNair, The thermal expansion of pure metals. Molybdenum, palladium, silver, tantalujm, tungsten, platinum, and lead, Physical Review 61 (1942) 74–78.
[23] F.A. Lewis, The Palladium Hydrogen System, Academic Press, London, 1967.
[24] F.A. Lewis, Hydrogen in palladium and palladium alloys, International Journal of Hydrogen Energy 21 (1996) 461–464.
[25] E. Lee, J. Lee, J. Koo, W. Lee, T. Lee, Hysteresis behavior of electrical resistance in Pd thin films during the process of absorption and desorption of hydrogen gas, International Journal of Hydrogen Energy 35 (2010) 6984–6991.

Biographies

Taehoo Chang was born in 1986 at Incheon, Republic of Korea. He received B.E. in material science and engineering at Yonsei University in 2012. He is currently studying on the hydrogen sensors based on MOTIFE and thermoelectric properties of Bi nanowires toward his M.E. degree at Yonsei University.

Hwaebong Jung was born in 1986 at Yesan, Republic of Korea. He received B.E. in material science and engineering at Yonsei University in 2012. He is currently studying on the MOTIFE sensor and hydrogen storage using Mg toward his M.E. degree in hydrogen storage and sensor devices at Yonsei University.

Byungjin Jang was born in 1987 at Seoul, Republic of Korea. He received B.E. in Material science and engineering at Yonsei University in 2012. He is currently studying on the MOTIFE sensor using Pd towards his M.E. degree in Hydrogen sensor devices at Yonsei University.

Junmin Lee received his M.S. from Materials Science and Engineering Department of Yonsei University in 2010. His research interest is to fabricate nanosensors using nanomaterials, etc. He is a doctoral student in the Department of Materials Science and Engineering at University of Illinois at Urbana-Champaign.

Jin-Seo Noh earned his bachelor's degree in 1991, master's degree in 1993 from Korea University, Korea, and Ph.D. degree in materials science in 2003 from University of Wisconsin–Madison. He has been with the Samsung Advanced Institute of Technology (SAIT) as a member of research staff in 2003–2008, where he performed research on next-generation memories and logic devices. He spent another one year and two months working on 28 nm technology development at the System LSI Division of Samsung Electronics. In 2009, he was appointed as a research professor to the Institute of Nanoscience and Nanotechnology of Yonsei University. His current research interests include nanomaterials-based thermoelectric energy conversion, nano electronics/spintronics, nanostructures-utilizing hydrogen gas and toxic gas sensors, and technology fusion crossing the borders.

Wooyoung Lee is a professor of Department of Materials Science and Engineering, the chairman of Yonsei Institute of Convergence Technology and the Head of Institute of Nanoscience and Nanotechnology at Yonsei University in Korea. He received a BS degree in metallurgical engineering in 1986, a MS degree in metallurgical engineering from the Yonsei University in 1988. He received a Ph.D. degree in physics from University of Cambridge, England in 2000. He is also the director in Korea-Israel Industrial R&D Foundation and the advisor in National Assembly Research Service. In recent years, his research interests have centered on thermoelectric devices, spintronics, hydrogen sensors and hydrogen storage materials. He has received a number of awards in nano-related research areas and a Service Merit Medal (2008) from the Korean Governments due to contribution on the development of intellectual properties. He has authored and co-authored over 150 publications, and has edited a few of special books on nano-structured materials and devices.